Acta Montanistica Slovaca
ISSN 1335-1788
actamont.tuke.sk

Complex determination of automatic robotic total stations' measurements' accuracy in underground spaces and comparison with results on the surface

Hana BRAUNOVÁ[1], Jaroslav BRAUN[2], Hana VÁCHOVÁ[3] and Ivan KURIC[4]*

Authors' affiliations and addresses:
[1] Department of Special Geodesy, Faculty of Civil Engineering, Czech Technical University in Prague, Thákurova 7, 166 36 Prague 6, Czech Republic
e-mail: hana.braunova@fsv.cvut.cz

[2] Department of Special Geodesy, Faculty of Civil Engineering, Czech Technical University in Prague, Thákurova 7, 166 36 Prague 6, Czech Republic
e-mail: jaroslav.braun@fsv.cvut.cz

[3] Department of Special Geodesy, Faculty of Civil Engineering, Czech Technical University in Prague, Thákurova 7, 166 36 Prague 6, Czech Republic
e-mail: hana.vachova@fsv.cvut.cz

[4] Faculty of Mechanical Engineering and Computer Science, University of Bielsko-Biala, ul. Willowa 2, 43-309 Bielsko-Biala, Poland
e-mail: kuric.ivan@gmail.com

***Correspondence:**
Hana Braunová, Department of Special Geodesy, Faculty of Civil Engineering, Czech Technical University in Prague, Thákurova 7, 166 36 Prague 6, Czech Republic
tel.: +420-22435-4780
e-mail: hana.braunova@fsv.cvut.cz

Funding information:
Grant Agency of CTU in Prague.
SGS23/049/OHK1/1T/11

Acknowledgement:
This research was funded by the Grant Agency of CTU in Prague – grand number SGS23/049/OHK1/1T/11 "Optimization of acquisition and processing of 3D data for purpose of engineering surveying, geodesy in underground spaces and 3D scanning"

How to cite this article:
Braunová, H., Braun, J., Váchová, H. and Kuric, I. (2023), Complex determination of automatic robotic total stations' measurements' accuracy in underground spaces and comparison with results on the surface, *Acta Monstanistica Slovaca*, Volume 28 (3), 752-764

DOI:
https://doi.org/10.46544/AMS.v28i3.18

Abstract
The total station is the most basic geodetic measuring instrument, locally the most accurate and versatile. Its accuracy is the cornerstone of its use and is defined by the standard deviations of horizontal direction, zenith angle and slope distance measurements. These accuracy parameters are given by the manufacturer, but these are only valid under optimum measurement conditions. To ensure the credibility and reliability of the measurements, these values must be periodically ascertained or determined for atypical measurement configurations or measurement conditions. Standardised procedures are used for this purpose, but in our opinion, they do not reflect the full influence of the measuring conditions and other measuring aids. A comprehensive determination of the accuracies (variation components) from the alignment, where all possible influences in a given situation are applied, may be considered the most appropriate for determining the angular accuracy of measurements. Such atypical conditions are certainly represented by geodetic measurements in the confined spaces of an underground mine. Thus, an experimental determination of the accuracy of four different robotic total stations was carried out at the Center of experimental geotechnics in a mine Josef teaching centre (CTU in Prague), and the Förstner method was used to determine the variation components. A network of 6 stations and 8 target points was designed. The grid size was approximately 32x21 m with 4 - 31 m lengths. A network with the same configuration was also duplicated at the surface to assess whether the accuracy is different in underground and how the results will correspond to the accuracy claimed by the manufacturers. The result of the testing is that the accuracy claimed by the manufacturers is maintained even under such difficult measurement conditions in narrow corridors and with short sights. The overall evaluation also found that the accuracy achieved underground and on the surface is identical, although it varies from instrument to instrument.

Keywords
Geodetic network, total station, variation components, least squares adjustment, Förstner's method, automatic targeting, robotic total station, standard deviation

Introduction

The Total Station is a basic geodetic instrument that, even in the era of 3D scanners, drones, and global satellite navigation systems, represents the most versatile and accurate method of spatial geometric measurement, achieving accuracy in low millimeters in areas of kilometers. At the same time, they do not need other objects to function. They are not limited by signal or space to fly; they work in principle equally on the construction site, in free space, in the forest, in a tunnel, or in the mine. However, the condition for proper functioning is the metrological correctness of the measured quantities, which must be regularly verified. This is important in many applications, such as in applications determining the shape and size of large machinery (Maisano et al., 2023), (Kovanič et al., 2020), (Bartoš et al., 2019), (Mogilny & Sholomitskii, 2017); monitoring of building objects' deformations (Mukupa et al., 2016), (Ehrhart & Lienhart, 2015), (Głowacki, 2022); landslides (Artese & Perrelli, 2018), (Urban et al., 2019) or general monitoring procedures (Vaněček & Štroner, 2016), (Bauer & Lienhart, 2023).

A very specific area with a requirement for high precision of measurement is the engineering surveying in underground spaces, where it is usually measurements during tunneling (Urban & Jiřikovský, 2015), (Bryn et al., 2017), (Nuttens et al., 2014), (Luo et al., 2016) or measuring and calculating volumes before and after mining (Štroner, 2019).

However, the use of total stations is also indirectly reflected in several fundamental scientific works on mass data collection. For the method of photogrammetry, it is necessary to determine the exact dimension and georeference through ground control points (Štroner et al., 2021), (Padró et al., 2019), (Kovanič et al., 2023). Furthermore, it serves for selective determination of the accuracy of point clouds (Peppa et al., 2019), (Moudrý et al., 2019) and determining the precision of detected surfaces and volumes (Kovanič et al., 2021) and the quality of the created digital terrain model (Forlani et al., 2018). For the use of laser 3d scanning, it is also necessary to determine the coordinates of ground control points, e.g., for geohazard monitoring (Kovanič et al., 2020), mobile or aerial scanning (Kalvoda et al., 2020) (Jon et al., 2013) or for measurements for the needs of heritage (Koska et al., 2013). In many cases, however, measurement using a precise total station serves to determine the benchmark in order to compare other measurement methods in terms of accuracy and thus also indirectly determine their usability or reliability, e.g., airborne laser sensors (Štroner et al., 2021), (Fuad et al., 2018), (Koska & Křemen, 2014). Last but not least, knowing the correct values of the a priori standard deviations of the instrument's measured values are also necessary for the correct adjustment of geodetic networks for the use of the robust methods for removing remote measurements (Štroner et al., 2014), (Gašincová & Gašinec, 2010), (Karsznia et al., 2023), (Sisman et al., 2012), (Třasák & Štroner, 2014) or their optimization (Amiri-Simkooei & Sharifi, 2004) (Yetkin et al., 2008) (Štroner et al., 2017) (Berne & Baselga, 2004).

The accuracy of total stations is described by standard deviations in determining the horizontal direction (σ_φ), zenith angle (σ_ζ), and slope distance (σ_{sd}). It is possible to estimate them separately as described in technical standards (e.g. (ISO 17123, 2005)) or through alternative or partial procedures (Lambrou & Nikolitsas, 2015), (Braun, 2015); (Gmitrowicz-Iwan et al., 2011). These are mainly based on repeated measurements (in the case of horizontal directions and zenith angles or comparing measured values with a reference value (determined with significantly higher accuracy) in the case of slope distances (Lechner, 2008). However, these methods are not carried out under real measurement conditions, and no additional environmental influences are inseparable from geodetic measuring. These methods are, therefore, in our opinion, suitable for the determination of accuracy under ideal conditions, but under real conditions, it is necessary to consider the possible deterioration of precision characteristics. Thus, more suitable for practical use (e.g., precision planning or optimization of geodetic measurements) can be considered methods of complex (simultaneous) accuracy determination, where the measurement is carried out under real conditions and all influences, including, for example, the non-linear propagation of light in the atmosphere, are reflected in the results. (Suk & Štroner, 2021).

The most statistically reliable known method of determining the previously mentioned accuracy characteristics is from the least squares adjustment of the geodetic network with the application of Förstner's method to determine the variation components with as many redundant measurements as possible.

Due to the absence of satellite signals underground, the total station measurement is practically the only realistic way to determine the coordinates of geodetic points accurately, and therefore, the accuracy of total station measurements underground is critical. Given the generally more difficult and different conditions (e.g., narrow corridors, different arrangement of atmospheric temperature layers) in mining measurements, the aim is to compare the accuracy achieved in underground mine and surface measurement (under "normal" conditions) with the fact that the shape and size of both test geodetic networks are identical. Since the accuracy is usually tested on the surface only, the aim is also to verify whether the accuracy claimed by the manufacturers is also met underground. In practical measurements, automatic targeting is commonly used when measuring surveying networks signalized by the reflective prisms, so it will also be used here.

Material and Methods

A process using geodetic networks with fixed target points and free stations has been proposed for the method of complex testing of automatic targeting and measurement of robotic total stations. Within the geodetic network, horizontal directions, zenith angles, and slope distances are repeatedly automatically measured in groups to other network points signaled by the reflective prisms. The configuration of the network and the number of points can be changed according to local conditions, but it must be optimized to ensure sufficient redundant values for the least squares adjustment and application of Förstner's method of determining variation components (Förstner, 1979).

Instruments

Four robotic total stations were selected for the test measurement: the Leica TS60, Leica MS60, Trimble S9HP, and Trimble S6HP (Fig. 1). The standard deviations indicated by the manufacturers are shown in Table 1. All devices are used and are regularly serviced. All total stations are used for very precise measurements in engineering surveying.

Tab. 1. Robotic total station measurement standard deviations given by manufacturers

Standard deviation / Total station	Leica TS60	Leica MS60	Trimble S9HP	Trimble S6HP
σ_{φ}	0,15 mgon	0,3 mgon	0,3 mgon	0,3 mgon
σ_{ζ}	0,15 mgon	0,3 mgon	0,3 mgon	0,3 mgon
σ_{sd}	0,6 mm + 1 ppm	1 mm + 1,5 ppm	0,8 mm + 1 ppm	1 mm + 1 ppm

The Leica and Trimble instruments were chosen because of their different ways of performing automatic targeting. The Leica instruments are equipped with an image detector for automatic targeting. The image detector works on the principle of a CCD (CMOS) sensor, where the position of the incident electromagnetic radiation is evaluated on the sensor matrix, and the aiming line of the instrument's telescope is directed to the center of the evaluated position. Trimble instruments are equipped with a quadrant auto-targeting detector. The quadrant detector works on the principle of light-sensitive diodes, where the intensity of the incident electromagnetic radiation is evaluated in each field, and the telescope is directed to the target so that the intensity of the incident radiation is the same in all four fields of the detector (Ehrhart & Lienhart, 2017)

Fig. 1. Total stations tested – a) Leica MS60, b) Trimble S9HP c) Trimble S6HP d) Leica TS60

Location and test networks

Test measurements were carried out in two locations. The primary site was in the underground Josef mine, which is the Center of experimental geotechnics (CEG) – an underground experimental center of the Faculty of Civil Engineering of the Czech Technical University in Prague (Fig. 2). It is located about 50 km south of Prague near the Slapy dam (between the villages of Čelina and Mokrsko in the Příbram region). It was excavated in 1981-91 as part of the geological exploration of gold-bearing deposits. The Faculty of Civil Engineering of the Czech Technical University in Prague opened the CEG here in 2007. The main underground corridor passes through the SSW direction through the rock mass of Veselý vrch. The corridor is followed by other linear exploration tunnels with numerous grooves tracing ore structures partly with connections to the other 2 floors. The vast majority (around 90%) of the breaches are not reinforced. A 136 m high unreinforced ventilation stack connects the end of the spine adit to the ground surface. The total length of the passages is 7853 m. The main corridor is 1835 m long

with a 14-16 m2 profile. The other corridors are 6018 m long in total, with a mean profile of 9 m^2. The height of the overburden is 90-150 m. (CEG, 2014)

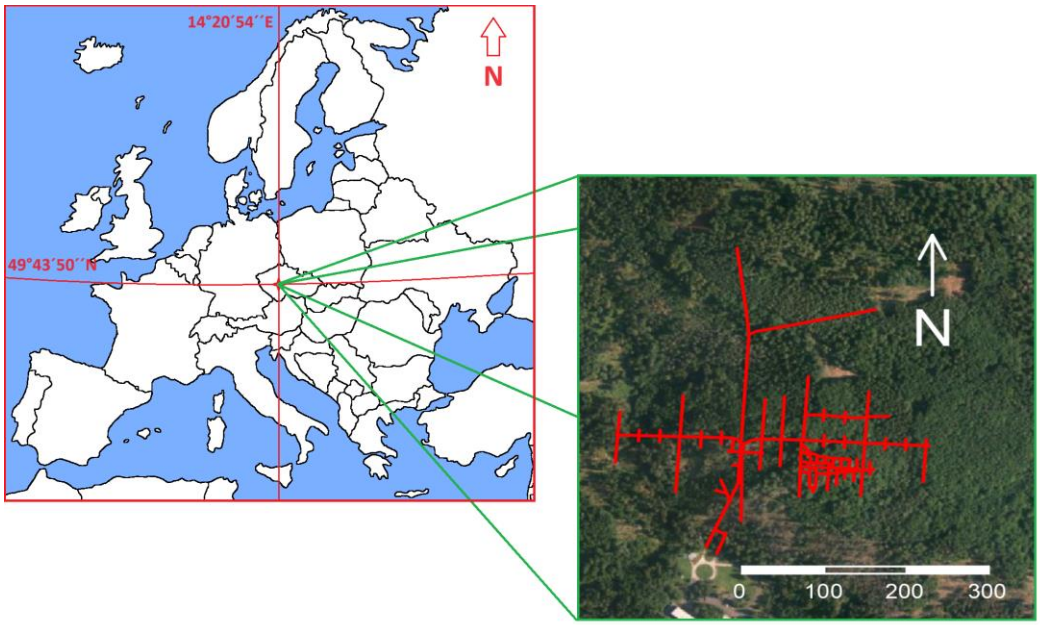

Fig. 2. Location CEG – Josef mine in Czech Republic

In this area, it was necessary to design a geodetic network with enough redundant measurements, i.e., interconnected corridors (visibility is necessary, full throughput is not necessary). Here, the target points were stabilized, and the positions of the free survey stations were designed so that the maximum number of target points from each station could be measured. Furthermore, the lengths of the intents are approximately equal in length (ideally within a 2:1 ratio), while at the same time not appearing too short in side lengths (up to about 2m), which can cause difficulties in targeting.

The three sides of the quadrangle were formed in standard corridors 2.2 m wide and 2.6 m high. The fourth side of the quadrangle was located in the area, which is an 8 m wide, 9 m to 22 m long and 39 m high chamber with a sloping rubble surface (Fig. 3). The target points consisted of 30 mm diameter spherical prisms placed in cylindrical nests mounted on a Zeiss tripod (Fig. 4). The spherical prisms were chosen to minimize the effects of the eccentricities of the surveying tools, which can be as small as a few tenths of millimeters (Braun & Štroner et al., 2016). A total of 8 target points (two in each vertex) were monumented in the corners of the quadrilateral. For the points closer to the center of the quadrilateral, the tripods were placed at a minimum height of approx. 1.0 m. In the case of the outer points, the tripods were set to a height of approx. 1.5 m to increase the height distribution. A total of 6 positions were chosen; the whole arrangement is shown in Fig. 3. Within each side, there was one position approximately in the middle. The other two positions were located at the corners of the corridors, from where visibility into the adjacent corners of the quadrangle was possible. The position in the middle of the side that runs through the cathedral was 1.5 m higher than the others because of the rubble embankment. The total size of the network was 32 m x 21 m, and the lengths ranged from 4 m to 31 m. At standpoint 1 (in the middle of the side passing through the cathedral), the lengths of intention were 7.7 m - 12.2 m. At standpoint 2 (midway along the side), the lengths of the intentions were 13.0 m - 16.2 m. At standpoint 3 (at the corner of the grid), the lengths of the intentions were 21,2 m - 31,3 m. At standpoint 4 (middle of the side), the lengths of intent were 9,2 m - 14,3 m. At standpoint 5 (at the corner of the grid), the lengths were 9,2 m - 25,4 m. At standpoint 6 (mid-side), the lengths of intent were 4,0 m - 7,0 m.

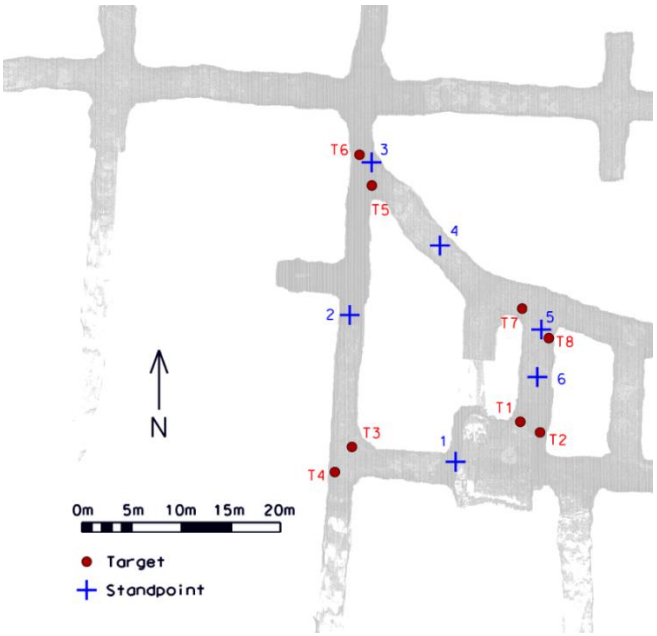

Fig. 3. Scheme of the network

Fig. 4. Josef URC – experimental network, standpoint 6 (left), detail of the reflective prism (right)

The site chosen for the surface measurements was a meadow near the village of Řisuty u Slaného (Fig. 5). This area resembles an underground site in its height and size. It consists of a continuous grassy area that helps maintain the same atmospheric conditions. The same network configuration as in the underground was implemented within the site with the same prisms and other accessories. All staked out with centimeter accuracy.

Fig. 5. Surface location - experimental network, standpoint 5

Description of the experiment

The experimental measurements at both sites were identical. First, the target points were monumented by carefully positioned tripods, then mounting the tripods with nests and placing them in the spherical prisms was performed. Each target point had its own reflective prism. Prisms were carefully oriented with respect to the total station each time the instrument was moved to suppress resulting targeting errors (Lackner & Lienhart, 2016). In addition, the positions of the stations were staked out. All 6 standpoints were always measured by each tested instrument in immediate succession. Each instrument was tempered to ambient temperature for at least 30 min before measurement. Each instrument was then electronically tempered by 25 groups of automatic measurements in both telescope positions (faces) on 1 target. This method of tempering is useful to stabilize the inner electronic components' temperature and suppress initial errors in the measurement data. During the measurements, atmospheric characteristics (temperature, air pressure) were measured and entered into the total station to calculate the measured distance's physical correction automatically. During the underground measurements, conditions were constant with a temperature of 10°C and atmospheric pressure of 978 hPa. During the surface measurements, it was cloudy and windless, which helped to maintain stable conditions with a temperature of 17°C and an atmospheric pressure of 982 hPa. Stability of conditions is an important condition for achieving objectively comparable results (Woźniak & Odziemczyk, 2017). Since one type of target prism was used, all total stations were set to the absolute additive constant given by the manufacturer (-11.3 mm). A tripod was always carefully set up at each station, and the total station was carefully mounted using an electronic level. The measurements were always made using software for measuring the set of directions in groups. The automatic measurements were made in 6 groups in total; the first group was excluded from the processing due to the operator's contact with the instrument during the definition of the measured points (the first face of the first group). The measurement scheme A'B'B"A" was followed. That is, within one group, first, all points in the first position of the telescope (face) were measured, and then, in reverse order, all points in the second position of the telescope (face) were measured. The differences between the groups were checked in the instrument program immediately after the measurements. Each of the total stations was set in standard precision measurement mode. Individual observations were exported for angles with a resolution of 0.01 mgon and for lengths with a resolution of 0.1 mm. Further used data for evaluation are the results of measurements from each group (average of two telescope positions), i.e., horizontal directions, zenith angles, and slope distances.

Evaluation methodology

The evaluated data are the results of measurements from each group (average of two telescope positions), i.e., horizontal directions, zenith angles, and slope distances. The basic principle of the evaluation is based on the least squares adjustment of the free 3d network. The main idea of least squares adjustment is to minimize the weighted sum of the squares of the measurement corrections in the calculation. The key condition of this method can be generally stated (according to (Böhm et al., 1990)):

$$\boldsymbol{v}^{\boldsymbol{T}} \cdot \boldsymbol{P} \cdot \boldsymbol{v} = min, \tag{1}$$

where **v** is the vector of corrections assigned by the measurements, and **P** is the weight matrix of the measured values. The corrections **v** are defined as the difference between the vector of adjusted measured values $\bar{l}(x)$ and the vector of the directly measured values **l**. The correction equation can be written as:

$$\boldsymbol{v} = \bar{\boldsymbol{l}}(x) - \boldsymbol{l}. \tag{2}$$

Measurements vector:

$$\boldsymbol{l} = (\boldsymbol{l_{sd}}\,;\ \boldsymbol{l_{\varphi}}\,;\ \boldsymbol{l_{\zeta}}). \tag{3}$$

The unknown values in the adjustment are the coordinates of all network points (X, Y, Z) and the orientation shifts of the horizontal directions measured at the position points of the network (op). The vector of unknowns where *n* is the number of points in the network and *k* is the number of standpoints can be written:

$$\boldsymbol{X} = (X_1\ \ X_2\ \ \cdots\ X_n\ \ Y_1\ \ \cdots\ Y_n\ \ Z_1\ \ \cdots\ Z_n\ \ op_1\ \ \cdots\ op_k)^T. \tag{4}$$

The relationships providing the functional dependence between the measured and unknown variables or the so-called observation equations can be expressed as:

$$sd_{ij} = \sqrt{(X_j\text{-}X_i)^2 + (Y_j\text{-}Y_i)^2 + (Z_j\text{-}Z_i)^2}, \quad (5)$$

$$\varphi_{ij} = \arctan\left(\frac{Y_j\text{-}Y_i}{X_j\text{-}X_i}\right)\text{-}op_i + o_K, \quad (6)$$

$$\zeta_{ij} = \arccos\left(\frac{z_j\text{-}z_i}{(X_j\text{-}X_i)^2+(Y_j\text{-}Y_i)^2+(z_j\text{-}z_i)^2}\right). \quad (7)$$

where *i* denotes the position, *j* the target, op_i the orientation shift on the relevant standpoint and o_K correction to the correct quadrant.

From the above equations (5), (6), (7), it is clear that the relationships between measured values and unknowns are not linear. This requires linearization, which can be done using the Taylor series with restrictions to first-order derivatives only:

$$\bar{x} = x_0 + dx, \quad (8)$$

$$v = \bar{l}(x_0) + \frac{\partial \bar{l}(x)}{\partial x}|_{x=x_0} \cdot dx\text{-}l \quad (9)$$

A correction equation can be written as:

$$\boldsymbol{A} = \frac{\partial \bar{\boldsymbol{l}}(\boldsymbol{x})}{\partial \boldsymbol{x}}|_{\boldsymbol{x}=\boldsymbol{x_0}}, \bar{x} = x_0 + dx \quad (10)$$

$$\boldsymbol{l'} = \bar{\boldsymbol{l}}(x_0) - \boldsymbol{l} \quad (11)$$

$$v = A \cdot dx + l' \quad (12)$$

where $\mathbf{x_0}$ is a vector of approximate values of unknowns, $d\mathbf{x}$ is a vector of updates of approximate values of unknowns, $\mathbf{l'}$ is a vector of reduced measurements, $\bar{\mathbf{l}}(x_0)$ is a vector of "measured" values calculated by observation equations using approximate unknows x_0 (5), (6), (7), and **A** is a matrix of partial derivatives of the observation equations according to unknowns. Matrix **A**:

$$\boldsymbol{A} = \begin{bmatrix} \boldsymbol{A_{sd}} \\ \boldsymbol{A_{\varphi}} \\ \boldsymbol{A_{\zeta}} \end{bmatrix}, \quad (13)$$

The calculation is solved by the adjustment of a free network, which is not georeferenced in the space, i.e., the coordinates of all points of the network are considered to be unknown and are to be the result of the adjustment. Positioning in the space is carried out by the point-zimuth method. This method sets the conditions for unknowns in the form of one fixed point and one fixed azimuth.

From the partial derivatives of the individual conditions according to the individual unknown, a matrix B is created, which is called the matrix of linearised conditions. The matrix has 4 rows (representing X, Y, Z, and the azimuth) and a number of columns corresponding to the number of unknowns. The matrix is made up of 0 and 1, which are at the position of a fixed point, and the derivatives of the director (coordinate difference / square of distance) between two selected points.

Measured data entering the adjustment with different accuracy, and it is necessary to consider this fact in the calculation by introducing the weights given for the individual measurements:

$$p_i = \frac{{\sigma_0}^2}{{\sigma_i}^2}, \quad (14)$$

where σ_0 is a priori standard deviation = selected constant $\sigma_0 = 1$. A σ_i is the a priori standard deviation of the measured value (i.e., the apriori standard deviation of measured slope distance σ_{sd}, the apriori standard deviation of a measured horizontal direction σ_{φ}, and the apriori standard deviation of a measured zenith angle σ_{ζ}). According to the formula (14), the weights of each measurement can be calculated, and the diagonal weight matrix **P** can be compiled from them:

$$P = \begin{bmatrix} p_{sd_1} & 0 & 0 & 0 \\ 0 & p_{sd_2} & 0 & 0 \\ 0 & 0 & \ddots & 0 \\ 0 & 0 & 0 & p_{\zeta_m} \end{bmatrix}.. \quad (15)$$

Using matrices **A**, $\mathbf{l'}$, **B**, **P** and solving of the normal equations system, the updates of the unknowns $d\mathbf{x}$ are:

$$\begin{bmatrix} dx \\ k \end{bmatrix} = -\begin{bmatrix} A^T PA & B^T \\ B & 0 \end{bmatrix}^{-1} \begin{bmatrix} A^T Pl' \\ b \end{bmatrix}, \quad b = 0 \tag{16}$$

where **k** is a vector of supplementary unknowns (Lagrange's coefficients), **0** is a square matrix of zeros of size of number of conditions and **b** is a vector of absolute values of linearized conditions (closures).

Vector of adjusted unknowns – coordinates of points and orientation shifts – is calculated by adding the determined updates **dx** (according to (16)) to approximate values of unknowns x_0.

$$\bar{x} = x_0 + dx. \tag{17}$$

Variance-covariance matrix characterizing the adjusted unknowns:

$$M_{\bar{x}} = \sigma_0{}^2[\bar{Q}_{xx}], \tag{18}$$

s_0 is aposteriori standard deviation, given by:

$$s_0 = \sqrt{\frac{v^T \cdot P \cdot v}{n-u+p}}, \tag{19}$$

where n is the number of measurements, u is the number of unknowns, p is the number of georeferencing conditions. $\bar{\mathbf{Q}}_{\mathbf{xx}}$ is a part of the matrix of normal equations:

$$N^{-1} = \begin{bmatrix} A^T PA & B^T \\ B & 0 \end{bmatrix}^{-1} = \begin{bmatrix} \bar{Q}_{xx} & \bar{Q}_{kx}^T \\ \bar{Q}_{kx} & \bar{Q}_{kk} \end{bmatrix}. \tag{20}$$

Because there is a linearization of the observation equations in the calculation, it is necessary to perform the equation iteratively. In other words, in each step of the iteration, the resulting estimates of unknowns are placed equal to approximate values, and the entire calculation is done again.

This standard free network adjustment procedure is accompanied by the Förstner method, in which, in each step of the iteration, along with the change of approximate values, weights are also changed by defined indicative measurement standard deviations.

Iteration shall be performed as many times as the size of the a posteriori standard deviation s_0, determined by the equation (19), is sufficiently close to the value of the a priori standard deviation $\sigma_0 = 1$:

$$|s_0 - \sigma_0| < \varepsilon \quad . \tag{21}$$

In calculation, it is sufficient to use $\varepsilon = 0.0001$. The basic idea of estimating variation components by Förstner's method consists in calculating number of redundant measurements for individual groups of measured values separately. In contrast to the classical LSM, where all influences are mixed, and where only an aposterior estimate of the conformity of measurement corrections and the inserted weights characterizing the network as a whole is calculated, if the Förstner method is used, the aposterior standard deviation can be determined separately for the individual measurement groups, here for slope distances s_0^{sd}, for horizontal directions s_0^{φ} and for zenith angles s_0^{ζ}. The first step after the same leveling of the spatial network is the calculation of the redundant matrix **R**:

$$R = I - A\,\bar{Q}_{xx}\,A^T P, \tag{22}$$

where **I** is a square unit matrix with a size corresponding to the number of measurements. Each element on the diagonal of the redundant matrix expresses the contribution of a particular measurement to the total number of redundant measurements in the network. Thus, it is possible to quantify the number of redundant measurements contributed by the individual measurement groups, thus determining the number of redundant measurements for the measured slope distances r_{sd}, horizontal directions r_{φ} and zenith angles r_{ζ}.

Subsequently, an a posteriori estimate of the accuracy of the measured slope distances, horizontal directions, and zenith angles can be calculated using their determined contributions:

$$s_0^{sd} = \sqrt{\frac{\sum(vv)_{sd}}{r_{sd}}}, \qquad s_0^{\varphi} = \sqrt{\frac{\sum(vv)_{\varphi}}{r_{\varphi}}}, \qquad s_0^{\zeta} = \sqrt{\frac{\sum(vv)_{\zeta}}{r_{\zeta}}}. \tag{23}$$

Calculated estimates of standard deviations by equation (23) shall further be used to calculate the new weight matrix **P**, and the adjustment shall be repeated until condition (21) is met.

A more reliable determination of the indicative deviations of the sloping lengths can be achieved by defining the size of the network by using a "precise" defined slope distance ($\widehat{sd}$) between 2 net points (one or more ones).

Subsequently, some of the above equations are adjusted, but the principle of calculating the equation remains the same. The measurement vector (3) shall be extended by this reference distance. Also, to the partial derivative matrix **A** (13), the reference slope distance has to be added:

$$\boldsymbol{l} = \left(\boldsymbol{l_{sd}};\ \boldsymbol{l_{\varphi}};\ \boldsymbol{l_{\zeta}};\ \widehat{sd}_{ij}\right), \tag{24}$$

$$\boldsymbol{A} = \begin{bmatrix} \boldsymbol{A_{sd}} \\ \boldsymbol{A_{\varphi}} \\ \boldsymbol{A_{\zeta}} \\ \boldsymbol{A_{\widehat{sd}}} \end{bmatrix}, \tag{25}$$

An important definition occurs when assembling the weight matrix **P**. The principle of weighting each measurement according to the formula (14) remains, but the distance indicating the dimension of the network ($\widehat{sd}$) must be given a large weight. In other words, the input accuracy of this distance must, therefore, be very high (i.e., a low value of the standard deviation of approximately 0.01 mm – 0.001 mm) in order for the distance to be considered almost flawless and really define the dimension of the entire network. Then, the weight matrix **P**:

$$\mathrm{P} = \begin{bmatrix} \mathrm{p}_{\mathrm{sd}_1} & 0 & 0 & 0 & 0 \\ 0 & \mathrm{p}_{\mathrm{sd}_2} & 0 & 0 & 0 \\ 0 & 0 & \ddots & 0 & 0 \\ 0 & 0 & 0 & \mathrm{p}_{\zeta_\mathrm{m}} & 0 \\ 0 & 0 & 0 & 0 & \mathrm{p}_{\widehat{\mathrm{sd}}_{\mathrm{ij}}} \end{bmatrix}. \tag{26}$$

The next calculation procedure is already similar to the previous case without the distance defining the dimension of the network ($\widehat{sd}$). The adjusted values of unknowns are considered approximate, the a posteriori estimate of the accuracy of the measured slope distances, horizontal directions, and zenith angles is considered to be the new input precision of the weight matrix, and the adjustment is carried out again. However, the weight of the distance defining the dimension of the network remains the same in every step of iteration, unchanging.

This procedure is indicated here only as information; additional distances must be measured much more accurately, and this is practically possible only with the use of a laser tracker in field conditions. Not having it, it was not used in the experiment.

In case of lower-quality reflective prisms not knowing their additive constant with the precision needed, those additive constants can also be added as adjusted unknowns to the calculation. Since it was not our case, it was not needed.

The entire calculation was done according to the procedures described in the Matlab R2023b environment.

Results

Measurements from the underground (Table 2) and surface (Table 3) sites were evaluated in the same and previously described manner. The calculation was carried out for each instrument with 360 input measured values (6 standpoints, 4 targets on each position, measurement in 5 groups - horizontal directions, zenith angles, sloping lengths). The number of unknowns for each device was 48 (14 points with XYZ coordinates and 6 orientation shifts).

Tab. 2. Standard deviations of robotic total stations measurement – an underground network

Standard deviation / Total station	Leica TS60	**Leica MS60**	**Trimble S9HP**	**Trimble S6HP**
s_0^{φ} [mgon]	0,11	**0,10**	**0,27**	**0,37**
s_0^{ζ} [mgon]	0,19	**0,16**	**0,26**	**0,22**
s_0^{sd} [mm]	0,09	**0,11**	**0,21**	**0,21**

An iterative calculation using Förstner's method for calculating the variation components determined the standard deviations in the measurement of the horizontal directions, zenith angles, and slope distances for 4 different robotic total stations – Leica TS60 and MS60, Trimble S6HP and S9HP was realized. The number of iterations for each device ranged from 4 to 8 (the accuracy indicated by the manufacturer was used in the first iteration).

Tab. 3. Standard deviations of robotic total stations measurement – surface network

Standard deviation / Total station	Leica TS60	**Leica MS60**	**Trimble S9HP**	**Trimble S6HP**
s_0^{φ} [mgon]	0,14	**0,09**	**0,19**	**0,32**
s_0^{ζ} [mgon]	0,19	**0,19**	**0,30**	**0,34**
s_0^{sd} [mm]	0,09	**0,13**	**0,22**	**0,23**

Discussion

The data presented in the tables can be evaluated statistically in several ways. It is appropriate to assess the conformity of the indicated indicative deviations of the measured horizontal directions and zenith angles with the data provided by the manufacturer (Table 1). There are only two values of 0.15 mgon and 0.3 mgon here; based on the number of redundant measurements using the Tau test (see (Bohm, 1990)) it is possible to determine the limit value for the 95% probability as a coefficient of 1.13; i.e., 0.17 mgon, and 0.34 mgon; for the 99% probability it is 1.19 and therefore 0.18 mgon & 0.36 mgon. The thus defined boundaries of conformity meet virtually all the observed values for a probability of 99%, except for a very small excess of 0.01 mgon for the zenith angles of the Leica TS60 (both underground and surface measurements) and for the Trimble S6 HP for the horizontal directions of underground measurement. Other determined values also meet the criterion for a 95% probability.

For the assessment of whether the accuracy of measurements underground or on the surface differed from one another due to the variability of the identified standard deviations and due to some significantly lower values than expected (especially for the Leica MS60, which, despite having an angle precision of 0.3 mgon reached virtually half of it), the total quadratic mean was used for all the angular standard deviations of measurements for one network and all the instruments together. If, for example, underground measurement conditions resulted in a worse accuracy, this would have to be reflected in all instruments and, therefore, reliably in this average value. For the underground network, the mean, standard deviation of angular measurement is 0.24 mgon, and for the surface network, it is 0.23 mgon. It indicates that comparable accuracy can be expected in underground mining conditions as in usually surface conditions.

The individual standard deviations themselves vary for instruments and conditions despite a considerable number of redundant measurements, approximately 100 for each determined standard deviation. Here, unfortunately, repeated measurements in five groups cannot be considered completely independent; for instance, not only atmospheric influences are constant, and therefore it can be assumed that the variation of the results corresponds to a smaller number of redundant measures. Here, in the future implementation of a similar experiment, we believe that preference should be given to fewer repetitions and more independent standpoints.

Separately, it is to comment on the indicated slope distance standard deviations since they are clearly below the declared accuracy of total stations. Because there is no significantly more accurate distance defining the entire dimension present in the adjustment, these are only random errors on very short distances and, as such, correspond to the experience of testing distance meters (Braun et al., 2015). Their total average standard deviations for the site are 0.16 mm and 0.18 mm (in the order of underground – surface). Therefore, there is again no indicated difference in the accuracy of measurement. In the case of using a laser tracker (for instance, Leica AT-400) to determine the reference length, the determined standard deviations would better describe the actual absolute slope distance accuracy of measurement.

Conclusions

In the experimental underground center of the Faculty of Civil Engineering, CTU in Prague, an experiment was carried out in order to determine the standard deviations of the measured values by the the robotic total stations Leica TS60, Leica MS60, Trimble S9HP and Trimbles S6HP. Förstner's method of determining variation components was used for evaluation. Comparative measurements were carried out on the surface test site.

The resulting standard deviations indicate that all instruments (with minor deviations) correspond in their accuracy to the parameters indicated by the manufacturers. The process of evaluation using Förstner's method of determining variation components has proved to be effective and reliable even within geodetic networks with a limited number of sights and in a spatially limited configuration of targets and standpoints. For any practical use, it is advisable to recommend fewer repetitions and a greater number of independent opinions, and also, if possible, the determination of one or more lengths in the geodetic network with significantly higher accuracy, which will allow to determine the more truly characteristics of the precision of length measurement.

Differences between underground and surface measurement precision were not observed.

References

Amiri-Simkooei, A., & Sharifi, M. A. (2004, February). Approach for Equivalent Accuracy Design of Different Types of Observations. *Journal of Surveying Engineering*, *130*(1), 1–5. https://doi.org/10.1061/(asce)0733-9453(2004)130:1(1)

Artese, S., & Perrelli, M. (2018, January 29). Monitoring a Landslide with High Accuracy by Total Station: A DTM-Based Model to Correct for the Atmospheric Effects. *Geosciences*, *8*(2), 46. https://doi.org/10.3390/geosciences8020046

Bartoš, K., Pukanská, K., Repáň, P., Kseňak, U., & Sabová, J. (2019, June 27). Modelling the Surface of Racing Vessel's Hull by Laser Scanning and Digital Photogrammetry. *Remote Sensing*, *11*(13), 1526. https://doi.org/10.3390/rs11131526

Bauer, P., & Lienhart, W. (2022, August 20). 3D concept creation of permanent geodetic monitoring installations and the a priori assessment of systematic effects using Virtual Reality. *Journal of Applied Geodesy*, *17*(1), 1–13. https://doi.org/10.1515/jag-2022-0020

Berne´, J. L., & Baselga, S. (2004, June 21). First-order design of geodetic networks using the simulated annealing method. *Journal of Geodesy*, *78*(1–2). https://doi.org/10.1007/s00190-003-0365-y

Böhm, J., Radouch, V., & Hampacher, M. (1990) Teorie chyb a vyrovnávací počet. Geodetický a kartografický podnik. *Praha*, 2. vydání, Praha. ISBN 80-7011-056-2.

Braun, J. & Štroner, M. (2016). Experimental Determination of the Eccentricity of Surveying Accessories. 6th International Multidisciplinary Scientific Geoconference SGEM 2016 Informatics, Geoinformatics,and Remote Sensing Volume II

Braun, J., Štroner, M., Urban, R., & Dvořáček, F. (2015, August 6). Suppression of Systematic Errors of Electronic Distance Meters for Measurement of Short Distances. Sensors, 15(8), 19264–19301. https://doi.org/10.3390/s150819264

Bryn, M., Afonin, D., Bogomolova, N., & Nikitchin, A. (2017). Monitoring of Transport Tunnel Deformation at the Construction Stage. Procedia Engineering, 189, 417–420. https://doi.org/10.1016/j.proeng.2017.05.066

CEG - Centre of experimental geotechnics. (2014). Faculty of Civil Engineering CTU in Prague. https://ceg.fsv.cvut.cz/; 30.10.2023.

ČSN ISO 17123-3 (2005): Optics and optical instruments - Filed procedures for testing geodetic and surveying instruments - Part 3: Theodolites. Czech normalisation institute.

ČSN ISO 17123-4 (2005): Optics and optical instruments - Filed procedures for testing geodetic and surveying instruments - Part 4: Electro-optical distance meters. Czech normalisation institute.

Ehrhart, M. & Lienhart, W. (2017). Object tracking with robotic total stations: Current technologies and improvements based on image data. Journal of Applied Geodesy, 11(3). http://dx.doi.org/10.1515/jag-2016-0043

Ehrhart, M., & Lienhart, W. (2015). Monitoring of civil engineering structures using a state-of-the-art image assisted total station. Journal of Applied Geodesy, 9(3), 174-182. https://doi.org/10.1515/jag-2015-0005

Forlani, G., Dall'Asta, E., Diotri, F., Cella, U. M. D., Roncella, R., & Santise, M. (2018, February 17). Quality Assessment of DSMs Produced from UAV Flights Georeferenced with On-Board RTK Positioning. *Remote Sensing*, *10*(2), 311. https://doi.org/10.3390/rs10020311

Förstner, W. (1979) Ein Verfahren zur Schätzung von Varianz- und Kovarianzkomponenten. Stuttgart: AVN 11-12/1979, s. 446-453.

Fuad, N. A., Ismail, Z., Majid, Z., Darwin, N., Ariff, M. F. M., Idris, K. M., & Yusoff, A. R. (2018, July 31). Accuracy evaluation of digital terrain model based on different flying altitudes and conditional of terrain using UAV LiDAR technology. *IOP Conference Series: Earth and Environmental Science*, *169*, 012100. https://doi.org/10.1088/1755-1315/169/1/012100

Gašincová, S., & Gašinec, J. (2010). Adjustment of positional geodetic networks by unconventional estimations. Acta Montanistica Slovaca, 15(1), 71.

Głowacki, T. (2022, March 23). Monitoring the Geometry of Tall Objects in Energy Industry. *Energies*, *15*(7), 2324. https://doi.org/10.3390/en15072324

Gmitrowicz-Iwan, J., Myszura, M., Olenderek, T., Ligęza, S., & Olenderek, H. (2021, September 26). The Influence of Target Properties on the Accuracy of Reflectorless Distance Measurements. *Sensors*, *21*(19), 6421. https://doi.org/10.3390/s21196421

Jon, J., Koska, B., & Pospíšil, J. (2013, February 13). Autonomous airship equipped by multi-sensor mapping platform. *The International Archives of the Photogrammetry, Remote Sensing and Spatial Information Sciences*, *XL-5/W1*, 119–124. https://doi.org/10.5194/isprsarchives-xl-5-w1-119-2013

Kalvoda, P., Nosek, J., Kuruc, M., Volarik, T., & Kalvodova, P. (2020, December 1). Accuracy Evaluation and Comparison of Mobile Laser Scanning and Mobile Photogrammetry Data. *IOP Conference Series: Earth and Environmental Science*, *609*(1), 012091. https://doi.org/10.1088/1755-1315/609/1/012091

Karsznia, K., Osada, E., & Muszyński, Z. (2023, August 18). Real-Time Adjustment and Spatial Data Integration Algorithms Combining Total Station and GNSS Surveys with an Earth Gravity Model. *Applied Sciences*, *13*(16), 9380. https://doi.org/10.3390/app13169380

Koska, B., Křemen, T., & Štroner, M. (2014, October 23) Bore-sight calibration of the profile laser scanner using a large size exterior calibration field, *Proc. SPIE 9245, Earth Resources and Environmental Remote Sensing/GIS Applications V, 92451Q* https://doi.org/10.1117/12.2067451

Koska, B., & Křemen, T. (2013, February 13). The combination of laser scanning and structure from motion technology for creation of accurate exterior and interior orthophotos of st. Nicholas baroque church. *The International Archives of the Photogrammetry, Remote Sensing and Spatial Information Sciences*, *XL-5/W1*, 133–138. https://doi.org/10.5194/isprsarchives-xl-5-w1-133-2013

Kovanič, U., Štroner, M., Blistan, P., Urban, R., & Boczek, R. (2023, July). Combined ground-based and UAS SfM-MVS approach for determination of geometric parameters of the large-scale industrial facility – Case study. *Measurement*, *216*, 112994. https://doi.org/10.1016/j.measurement.2023.112994

Kovanič, U., Blistan, P., Urban, R., Štroner, M., Blišťanová, M., Bartoš, K., & Pukanská, K. (2020, November 28). Analysis of the Suitability of High-Resolution DEM Obtained Using ALS and UAS (SfM) for the Identification of Changes and Monitoring the Development of Selected Geohazards in the Alpine Environment—A Case Study in High Tatras, Slovakia. *Remote Sensing*, *12*(23), 3901. https://doi.org/10.3390/rs12233901

Kovanič, U., Blistan, P., Štroner, M., Urban, R., & Blistanova, M. (2021, July 16). Suitability of Aerial Photogrammetry for Dump Documentation and Volume Determination in Large Areas. *Applied Sciences*, *11*(14), 6564. https://doi.org/10.3390/app11146564

Kovanič, U., Blistan, P., Urban, R., Štroner, M., Pukanská, K., Bartoš, K., & Palková, J. (2020, October 29). Analytical Determination of Geometric Parameters of the Rotary Kiln by Novel Approach of TLS Point Cloud Segmentation. *Applied Sciences*, *10*(21), 7652. https://doi.org/10.3390/app10217652

Lackner, S. & Lienhart W. (2016). Impact of Prism Type and Prism Orientation on the Accuracy of Automated Total Station Measurements. *Joint International Symposium on Deformation Monitoring (Vienna).*

Lechner, J., Červinka, L., & Umnov, I. (2008) Geodetic Surveying Tasks for Establishing a National Long Length Standard Baseline Integrating Generations FIG Working Week 2008 Stockholm, Sweden 14-19 June 2008

Luo, Y., Chen, J., Xi, W., Zhao, P., Qiao, X., Deng, X., & Liu, Q. (2016, April). Analysis of tunnel displacement accuracy with total station. *Measurement*, *83*, 29–37. https://doi.org/10.1016/j.measurement.2016.01.025

Maisano, D. A., Mastrogiacomo, L., Franceschini, F., Capizzi, S., Pischedda, G., Laurenza, D., Gomiero, G., & Manca, G. (2022, October 29). Dimensional measurements in the shipbuilding industry: on-site comparison of a state-of-the-art laser tracker, total station and laser scanner. *Production Engineering*, *17*(3–4), 625–642. https://doi.org/10.1007/s11740-022-01170-7

Mukupa, W., Roberts, G. W., Hancock, C. M., & Al-Manasir, K. (2016, April 15). A review of the use of terrestrial laser scanning application for change detection and deformation monitoring of structures. *Survey Review*, 1–18. https://doi.org/10.1080/00396265.2015.1133039

Nuttens, T., Stal, C., De Backer, H., Schotte, K., Van Bogaert, P., & De Wulf, A. (2014, July). Methodology for the ovalization monitoring of newly built circular train tunnels based on laser scanning: Liefkenshoek Rail Link (Belgium). *Automation in Construction*, *43*, 1–9. https://doi.org/10.1016/j.autcon.2014.02.017

Padró, J. C., Muñoz, F. J., Planas, J., & Pons, X. (2019, March). Comparison of four UAV georeferencing methods for environmental monitoring purposes focusing on the combined use with airborne and satellite remote sensing platforms. *International Journal of Applied Earth Observation and Geoinformation*, *75*, 130–140. https://doi.org/10.1016/j.jag.2018.10.018

Peppa, M. V., Hall, J., Goodyear, J., & Mills, J. P. (2019, June 4). Photogrammetric assessment and comparison of dji phantom 4 pro and phantom 4 rtk small unmanned aircraft systems. *The International Archives of the Photogrammetry, Remote Sensing and Spatial Information Sciences*, *XLII-2/W13*, 503–509. https://doi.org/10.5194/isprs-archives-xlii-2-w13-503-2019

Mogilny, S., & Sholomitskii, A. (2017). Precision Analysis of Geometric Parameters for Rotating Machines during Cold Alignment. *Procedia Engineering*, *206*, 1709–1715. https://doi.org/10.1016/j.proeng.2017.10.702

Sisman, Y., Dilaver, A., & Bektas, S. (2012). Outlier detection in 3D coordinate transformation with fuzzy logic. Acta Montanistica Slovaca, 17(1), 1.

Suk, T., & Štroner, M. (2021, June 30). The impact of the air temperature on measuring the zenith angle during the year in the ground layer of the atmosphere for the needs of engineering surveying. *Acta Polytechnica*, *61*(3), 476–488. https://doi.org/10.14311/ap.2021.61.0476

Štroner, M., Křemen, T., Braun, J., Urban, R., Blišťan, P., & Kovanič, L. (2019) Comparison of 2.5D Volume Calculation Methods and Software Solutions Using Point Clouds Scanned Before and After Mining. *Acta Montanistica Slovaca*, 296-306. ISSN 1335-1788.

Štroner, M., Michal, O., & Urban, R. (2017) Maximal precision increment method utilization for underground geodetic height network optimization. *Acta Montanistica Slovaca*, 22(1), 32-42. ISSN 1335-1788.

Štroner, M., Urban, R., & Línková, L. (2021, November 27). A New Method for UAV Lidar Precision Testing Used for the Evaluation of an Affordable DJI ZENMUSE L1 Scanner. *Remote Sensing*, *13*(23), 4811. https://doi.org/10.3390/rs13234811

Štroner, M., Urban, R., Rys, P., & Balek, P. (2014, December 16). Prague Castle Area Local Stability Determination Assessment by the Robust Transformation Method. *Acta Geodynamica Et Geomaterialia*, 325–336. https://doi.org/10.13168/agg.2014.0020

Štroner, M., Urban, R., Seidl, J., Reindl, T., & Brouček, J. (2021, March 31). Photogrammetry Using UAV-Mounted GNSS RTK: Georeferencing Strategies without GCPs. *Remote Sensing*, *13*(7), 1336. https://doi.org/10.3390/rs13071336

Třasák, P., & Štroner, M. (2014, April 5). Outlier detection efficiency in the high precision geodetic network adjustment. *Acta Geodaetica Et Geophysica*, *49*(2), 161–175. https://doi.org/10.1007/s40328-014-0045-9

Urban, R. & Jiřikovský, T. Accuracy analysis of tunneling measurements in UEF Josef. *15th International Multidisciplinary Scientific GeoConference SGEM 2015*. Sofia: STEF92 Technology Ltd., 2015. p. 35-42. ISSN 1314-2704. ISBN 978-619-7105-35-3.

Urban, R., Štroner, M., Blistan, P., Kovanič, U., Patera, M., Jacko, S., Ďuriška, I., Kelemen, M., & Szabo, S. (2019, July 24). The Suitability of UAS for Mass Movement Monitoring Caused by Torrential Rainfall—A Study on the Talus Cones in the Alpine Terrain in High Tatras, Slovakia. ISPRS International Journal of Geo-Information, 8(8), 317. https://doi.org/10.3390/ijgi8080317

Vaněček, J., & Štroner, M. (2016). Testing the accuracy of measured values in continuous long-term geodetic monitoring. *Acta Polytechnica*, 56(6), 478-491. https://doi.org/10.14311/AP.2016.56.0478

Moudrý, V., Urban, R., Štroner, M., Komárek, J., Brouček, J., & Prošek, J. (2018, September 10). Comparison of a commercial and home-assembled fixed-wing UAV for terrain mapping of a post-mining site under leaf-off conditions. *International Journal of Remote Sensing*, *40*(2), 555–572. https://doi.org/10.1080/01431161.2018.1516311

Woźniak, M. & Odziemczyk, W. (2017). Investigation of Stability of Precise Geodetic Instruments Used in Deformation Monitoring. Reports on Geodesy and Geoinformatics 104(1). http://dx.doi.org/10.1515/rgg-2017-0017.

Yetkin, İ., İnal, C., Yigit, C.O. (2008) Optimal Design of Deformation Monitoring Networks By Using PSO Algorithm Measuring the Changes. *13th FIG Symposium on Deformation Measurements and Analysis, 4th IAG Symposium on Geodesy for Geotechnical and Structural Engineering*, 12-15 May, Lisbon-Portugal.